Arabian Journal of Geosciences (2021) 14:1544
https://doi.org/10.1007/s12517-021-07984-6

ORIGINAL PAPER

Past and future prediction of land cover land use change based on earth observation data by the CA–Markov model: a case study from Duhok governorate, Iraq

Nabaz R. Khwarahm[1] · Peshawa M. Najmaddin[2] · Korsh Ararat[3] · Sarchil Qader[4,2]

Received: 29 January 2021 / Accepted: 14 July 2021

Abstract

Understanding land use land cover change (LULCC) dynamics is crucial for sustaining the integrity of structure and function of ecosystems. As such, frequent measuring and monitoring of LULCC are necessary. Over the last four decades, Duhok governorate in the north of Iraq has undergone sweeping changes caused mainly by anthropogenic factors (e.g. population growth). This study used geospatial techniques and the synergy Cellular Automata (CA)–Markov approach to quantify past, current and model the future changes of LULC. The maximum likelihood classifier (MLC) was employed to conduct classification for three consecutive-year Landsat imagery (i.e. 1988, 2008 and 2017). From the classified imageries, three LULC maps with several classes were created and then, change detection analysis was implied. The classified (1988–2008) and (2008–2017) LULC maps were incorporated into the hybrid model to predict LULC maps for 2017 and 2060, respectively. The classified 2017 LULC maps were used as a reference to validate the model output for 2017.

Relatively high accuracy agreements were achieved between the classified and the modelled maps (Kno= 0.8315, Klocation= 0.8267, Kstandard = 0.7978). The model classes estimated for 2060 compared to the classified 2017 LULC classes revealed that dense forest, sparse forest, agricultural land and barren area would decrease by −26.26% (from 327.08 to 241.08 km^2), −0.76% (from 2372.29 to 2355.82 km^2), −5.86% (from 973.21 to 916.27 km^2) and −10.03% (from 2918.9–2626.19 km^2), respectively. In contrast, the urban area would significantly increase by 271.19%, (from 161.99 to 602.19.8 km^2).

Dense forest in Duhok governorate has seen remarkable decline from 1988 to 2017, and future predictions demonstrated that the declining trend would continue. Dense forest would predominantly convert to sparse forest and barren areas, suggesting forest thinning and clearing. Urban areas were the most dynamic cover types that increased significantly between 1998 and 2017. This trend would continue to increase from 2.36% (2017) to 8.76% (2060). Urbanization would be predominantly at the cost of agricultural land and barren area. Information on spatiotemporal dynamics of LULCC has been proved as an effective measure for maintaining the integrity of the ecosystem components through sustainable planning and management actions.

Keywords LULC · CA–Markov · Iraq · GIS · RS

Responsible Editor: Biswajeet Pradhan

✉ Nabaz R. Khwarahm
khwarahm21302@alumni.itc.nl

[1] Department of Biology, College of Education, University of Sulaimani, Sulaimani, Kurdistan Region 334, Iraq

[2] Natural Resources Department, College of Agricultural Engineering Sciences, University of Sulaimani, Sulaimani, Kurdistan Region 334, Iraq

[3] Department of Biology, College of Science, University of Sulaimani, Sulaimani, Kurdistan Region 334, Iraq

[4] WorldPop, Geography and Environmental Science, University of Southampton, Southampton SO17 1BJ, UK

Introduction

Land use land cover (LULC) is an important component of the environmental systems. Any changes to LULC can cause many environmental and ecological problems at various spatial scales (Karki et al. 2018; Tolessa et al. 2017). LULC is continuously changing due to natural and artificial factors (Lambin and Meyfroidt 2011). Anthropogenic activities as an example of artificial factor make LULC change faster than in the past, for example, the transformation of natural habitats into agricultural land to sustain human livelihoods (Ramankutty and Foley 1999), agricultural land for urban development (Chen 2007; Tan et al. 2005; Xu et al. 2015) and

Published online: 28 July 2021

rural migration which have been identified as one of the main drivers of global environmental change (Habitat and ESCAP 2015; Hyandye et al. 2015). In addition, the world's population increased from 2 billion in 1830 to 7.6 billion in 2017 (Wu et al. 2011) and is expected to reach 8.6 billion in 2030 (UN 2017), with the majority of these trends are in urban areas. For this reason, many landscapes around the world have been disturbed (Lambin and Meyfroidt 2011) particularly in developing countries than the developed countries (Dewan and Yamaguchi 2009). Monitoring these changes is therefore crucial to improving the resources management in developing countries (Hasanlou et al. 2018).

Geospatial technologies, remote sensing (RS) data and geographic information system (GIS) are currently considered to be the most cost-effective and accurate source of information for the detection of changes in LULC (Corner et al. 2014; Dewan and Yamaguchi 2009; Jensen 1996; Ouyang et al. 2016) due to its availability at different spatiotemporal coverage (Wu et al. 2015). Applying RS data to detect changes in LULC is the process by which objects in the same area of interest are measured over time using satellite images (Chen 2007; Wu et al. 2011). In this context, the Landsat imagery are widely applied to study land cover land use changes (LULCC) and they have proven to be accurate (Gómez et al. 2016; Guan et al. 2011; Li et al. 2020; Pflugmacher et al. 2019; Su et al. 2012; Zhu and Woodcock 2014).

In addition, there are different models that can be used for LULCC simulation and modelling, such as statistical models (Al-sharif and Pradhan 2016; Alsharif and Pradhan 2014; Alsharif et al. 2015), evolutionary models (Rimal et al. 2018), cellular automata (CA) (Al-sharif and Pradhan 2015), Markov chain models (Khwarahm 2021; Khwarahm et al. 2020), convolutional neural network (CNN) (Seydi et al. 2020) and GIS-based modelling (Abdullahi and Pradhan 2016; Abdullahi et al. 2015). Amongst them, CA and Markov chain analysis and their integration model which is well known as CA–Markov model is the best option for effective quantitative simulation and prediction of LULC changes at different spatial scales (Rimal et al. 2017). For instance; the CA–Markov model was applied by Rimal et al. (2018) to explore the past, present and future changes in LULC in the central east part of Nepal. Their analysis has shown that the cultivated land has been the most affected by urban expansion over the period 1988 to 2016 and is expected to continue in the future. The total urban area was 40.53 km^2 in 1988, increased to 144.35 km^2 in 2016 and projected significant urban growth of 200 km^2 in 2024 and 238 km^2 in 2032. Similarly, Wang et al. (2020) applied the CA–Markov model to detect and predict land use and land cover changes in Kathmandu City in Nepal over two decades (from 1990 to 2010). Their results reveal that the Kathmandu district has lost 9% of its forests, 10% of its agricultural land and 77% of its water bodies over 20 years due to growing urban areas, rapid development and inadequate planning and significant migration from rural to urban areas.

According to the Intergovernmental Panel on Climate Change (IPCC) Report 2019 (Arneth et al. 2019), the Middle East region undergoes severe changes in LULC (e.g. desertification) due to increased land surface temperature and evapotranspiration and reduced precipitation in interaction with anthropogenic activities. As a result, Iraq (as part of the ME region) has been confronted with many challenges in LULC management since the last three decades due to declining economies, random urbanization, population growth, drought, biodiversity loss (Khwarahm et al. 2021a; Khwarahm et al. 2021b), desertification and a series of wars, so Iraq's land is under enormous pressure. The study of LULCC therefore plays an important role in better decision-making and improving future development actions without degrading the integrity of the environmental systems (i.e. assists sustainable development). Several studies have been conducted on LULCC in Iraq, such as land cover classification using a phenology-base methodology (Qader et al. 2016), effect of land surface temperature on LULC (Alkaradaghi et al. 2018), local land use land cover change in Duhok City (Ibrahim and Rasul 2017), effects of a series war on LULC instability (Gibson et al. 2015) and using a panchromatic highly spatial resolution to modify LULC classification methodology (Dibs et al. 2020). In Iraq, there have been limited studies addressing LULCC quantification and prediction (Hadeel et al. 2010; Hadi et al. 2014; Khwarahm et al. 2020).

Tracing the impact of urban change on sustainability through time can supply vital information required for sustainable urban progress, particularly in areas where anthropogenic and natural factors are a constant risk (Barredo and Demicheli 2003; Hassan and Kotval-K 2019). The Duhok governorate in Iraq was chosen to carry out this study because it has faced several environmental, political and economic threats to its quality and growth of life (Agha and Şarlak 2016; Natali 2013). In addition, the Duhok governorate has been impacted enormously by both the insurgency of the Islamic State of Iraq and Syria (ISIS), which began in June 2014 and the Syrian civil war, which began in 2011 (Kulaksiz 2015). The violence and insecurity associated with each of these two events have forced many people to flee their homes and displaced them to many Kurdish cities in the north of Iraq, particularly Duhok. These factors with the absence of an urban planning system posed huge pressure on the lands due to the increased need for housing and have been the main drivers of LULCC. To address the past, present and future LULCCs, adequate datasets with sophisticated approaches will be essential to develop an effective planning system for sustainable growth in the future. This study uses high-resolution satellite data to extract necessary datasets for this analysis and employs the CA–Markov model to simulate and predict LULCC in Duhok governorate, in the republic of Iraq. The study outputs provide invaluable information for conservation ecologists for protecting the integrity of the ecosystems, urban planner and decision makers.

Materials and methods

Study area

Duhok governorate is located in the north of Iraq, bordering Syria and Turkey, situated between latitudes 36°–37.5° N and longitudes 42°–44° E, with elevations >580 m above sea level (Fig. 1). This governorate is one of the four governorates of the Kurdistan region of Iraq (KRI) and covers an administrative area of 6872.56 km^2 with four main districts (Duhok, Amedi, Simele and Zakho). The geomorphology of Duhok is characterised by the high terrains, complex mountains, steep slopes and hills and the valleys giving way to plains in its west. The climate of the Duhok is influenced by the Mediterranean zone; characterised by hot and dry summers, and cold and wet winters (Najmaddin 2017), with the maximum temperature reaches 42°C in July and minimum reaches 3 °C, respectively (http://bot.gov.krd/duhok-province).

Historical satellite imagery

Satellite images (30 m spatial resolution and the least cloud cover) from Landsat 5 Thematic Mapper (TM) and Landsat 8 (OLI TIRS) of three historical years (1988, 2008 and 2007), were downloaded (Table 1) from the Earth Explorer portal of the United States Geological Survey (USGS) (https:/earthexplorer.usgs.gov).

Dataset pre-processing and classification

Liang et al. (2002) argued that in order to obtain accurate quantitative surface information from satellite data, applying radiometric and atmospheric corrections is necessary. The Fast Line-of-sight Atmospheric Analysis of Hypercubes ((FLAASH) settings of the ENVI 5.2 platform was employed to correct the radiometric and atmospheric noises within the used satellite images prior to the classification process. In the setting, the required coefficients were obtained from the metadata of the images. The imagery scenes were mosaicked with the same time window and year, and the study area was then extracted. For the purpose of accurate surface feature identification, various band combinations such as RGB 5, 4, 3 for OLI and RGB 4, 3, 2 for TM (OLI and TM sensors have different band settings) were made to facilitate training data collection for the image classification. In addition, during the delineation of the feature classes (training sites), historical and current expert knowledge on the physiography of the study sites and useful supplementary data were incorporated. The following LULC classes were identified: dense forest, sparse forest, agricultural land, urban area, barren area and water bodies (Table 2). For every target year, around 130 spectral signatures (training-sits) in small polygons formats were extracted from mosaicked images (Congalton and Green 2019). The MLC which is based on the probability of a certain pixel belonging to a similar spectral distribution or similar pixel aggregate was

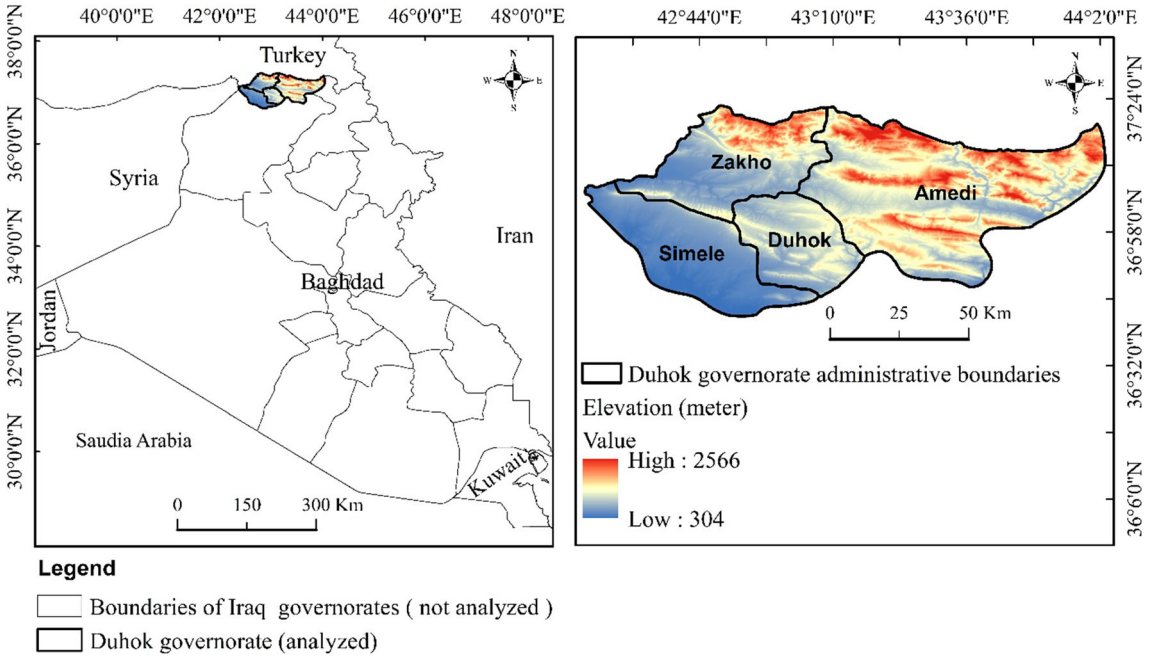

Fig. 1 Study site and administrative boundaries

Table 1 Description of the imagery used in the study

Path	Row	Latitude extent	Longitude extent	Bands used (RGB)	Acquisition time
169	34	36.40° N–38.53° N	43.43° E–46.09° E	432 (TM), 543 (OLI)	July 1988, July 2008 (TM); July 2017 (OLI)
169	35	34.96° N–37.10° N	43.03° E–45.64° E	432 (TM), 543 (OLI)	July 1988, July 2008 (TM); July 2017 (OLI)
170	34	36.37° N–38.55° N	41.86° E–44.56° E	432 (TM), 543 (OLI)	July 1988, July 2008 (TM); July 2017 (OLI)

applied with the spectral signatures to classify the image for each consecutive year. Three LULC maps were then generated with a spatial resolution of 30 m.

Classification assessment and change analysis

Accuracy assessment between automated classification data with reference data/ground control points is essential (Congalton and Green 2019). Thirty nine points out of 130 spectral signature samples (equivalent to 30% of the training dataset for each class) were randomly selected within a GIS environment using ArcMap 10.3 (Foody 2002). The accuracy of the 1988, 2008 and 2017 LULC maps resulting from the maximum probability classification was assessed by independent datasets. To do this, 234 points spreading across each LULC map for each year were generated based on an equalising random sampling technique, and then they were exported into Google Earth imagery as a 'shapefile' for identification and labelling. After that, the labelled points were used to create an error matrix with classified data (Rosenfield 1986; Van Oort 2007). From the error matrix, we then calculated the Kappa coefficient, overall accuracy and producer's and user's accuracy. After conducting the accuracy assessment for the generated LULC maps between 1988 and 2017, the quantification of the dynamics of changes for each target year 1988, 2008 and 2017 was investigated (i.e. by calculating the area of specific class category per time window (Butt et al. 2015)). Finally, cross-tabulation matrices (Jensen 1996; Pontius Jr and Cheuk 2006) were performed for change detection (Fig. 2 flow chart part A).

Markov Chain model, cellular automata (CA) model and CA–Markov models

The Markov chain model (MCM) depends on stochastic process which means that how random variable changes over time (Munthali et al. 2020) and the transition probability matrix (Koomen and Borsboom-van Beurden 2011). It has been widely accepted to simulate and predict future land-use change over time (Khwarahm et al. 2020). The predicted future LULCC usually depends on the transition probability matrix, transition area matrix of two time-period (i.e. t0 to t1) LULC maps. Therefore, MCM has demonstrated its ability to simulate LULC change whilst not providing the right spatial allocation and distribution of LULC change occurrences (Dbehera et al. 2012; Eastman 2012; Yang et al. 2012). On the other hand, the cellular automata (CA) model has the ability to represent non-linear and complex spatially distributed LULC's class category (Mishra and Rai 2016). The CA model consists of regular grid-cells with each grid in one of a finite number of states, and its main principle is that changes in cell status can be explained by current status and changes in surrounding cells based on the previous status (Guan et al. 2011; He et al. 2014; Liping et al. 2018). Therefore, the CA model can be applied to fill the gap of the spatial dimension limitation of the MCM (Khwarahm et al. 2020).

The CA–Markov is an effective combination between the MCM to predict temporal changes in LULC and cellular automata models to predict spatial LULCC, hence, the integrated CA–Markov model can be used

Table 2 Identified LULC classes from the satellite ixmagery and their interpretations

LULC class	Interpretation
Dense forest	Areas covered with oak trees (predominantly *Quercus aegilops*)
Sparse forest	Areas covered thinly with oak shrubs and tree (predominantly *Quercus aegilops*)
Agricultural land	Fertile areas used for agricultural activities ,predominantly for crops (wheat and barley)
Urban area	Man-made infrastructure (unnatural surfaces)
Barren area	Waste land and open areas predominantly with annual vegetation covers (e.g. grass)
Waterbody	Areas covered with water (natural and unnatural)

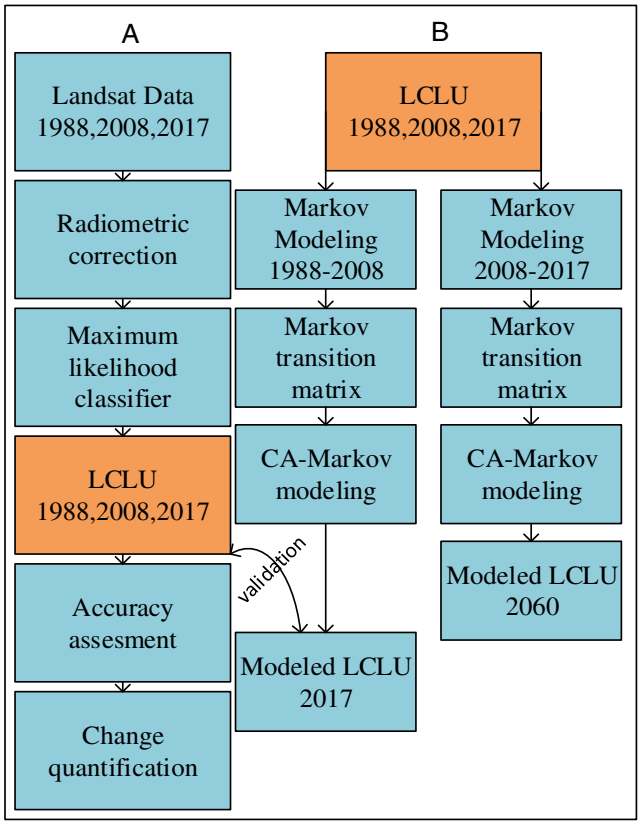

Fig. 2 Study flowchart (part A; represents LULC classification, accuracy assessment and change analysis, part B; represents CA–Markov validation and LULC modelling for 2060)

effectively to predict spatiotemporal changes in LULCC (Parsa et al. 2016). In this study, an existing modelling technique, the CA–Markov model in the IDRISI 17.0 was adopted to predict LULCC in the year 2060 for Duhok governorate based on the (1988–2008) and (2008–2017) LULC maps produced from the maximum likelihood classification after we were satisfied with the accuracy assessment (Fig. 2 part B).

Model validation

Model validation is a crucial step to evaluate the accuracy of predicted data. In this study, the validation was completed by using the classified 2017 LULC map as reference data against the predicted 2017 LULC map based on the standard Kappa index of agreement variations, which have been widely used to validate LULC predictions (Parsa et al. 2016). Kappa variations included the following: Kappa; (I) for location (Klocation); (II) for standard (Kstandard); (III) for locationStrata (KlocationStrata); and (IV) for no information (Kno) ((Pontius Jr 2000; Pontius Jr 2002; Pontius Jr and Millones 2011). Klocation and KlocationStrata measure the accuracy between reference and predicted map based on certain location and quantity of the LULC map (Pontius and Malanson 2005; Sayemuzzaman and Jha 2014). For the general agreement between proportions of the reference and modelled maps, regardless of having information on the quantity location of certain class categories, Kno is calculated. Kstandard is determined to assess the proportion of the class category that has been correctly correlated by chance. The Kappa values for these variations range from (0 to 1). The accuracy of the agreement is better if the value is closer to 1(Christensen and Jokar Arsanjani 2020).

Results

Land cover maps and accuracy assessment of the classification

The proposed method produces LULC map of Duhok governorate for 1988, 2008 and 2017 (Figs. 3, 4 and 5). Confusion matrix and the maximum likelihood classification techniques used to estimate the classification accuracy. The overall accuracy and Kappa coefficient calculated from 234 points for the target years are listed in Tables 3, 4 and 5. The overall kappa coefficients for the consecutive years 1988, 2008 and 2017 were 0.86, 0.89 and 0.92 respectively. The producer and user accuracies for 1988 LULC map were ranged from 0.83 to 0.94, whilst for the 2008 and 2017 LULC were ranged from 0.83 to 1.

Spatial analysis of LULC change classification

The LULC changes were spatially analysed. As shown in Table 6, the land cover/land use classes have changed between the period 1988, 2008 and 2017. For instance, between the period 1988–2008, the dense forest and waterbody have decreased by −42.91% (860 km^2 to 491 km^2) and −19.08% (152 km^2 to 123 km^2) respectively, whilst during that period, the sparse forest, agricultural land, urban area and barren area have increased by 13.33%, 16.8%, 16.22% and 2.43% respectively. LULC changes during the period 2008–2017 are slightly different from the period (1988–2008). During that period, the sparse forest has slightly increased by 1.47% whilst, agricultural land and urban area have significantly increased by 223.2% (300 km^2 to 973 km^2), and 448.84% (29 km^2 to 161 km^2) respectively. In contrast, the dense forest, barren area and waterbody have decreased by −33.43%, −18.69% and −3.35%, respectively (Table 6).

Comparison between actual LULC and modelled LULC map of 2017

The degree of agreement between the actual LULC map and the modelled LULC map for the 2017 was R^2 = 0.98

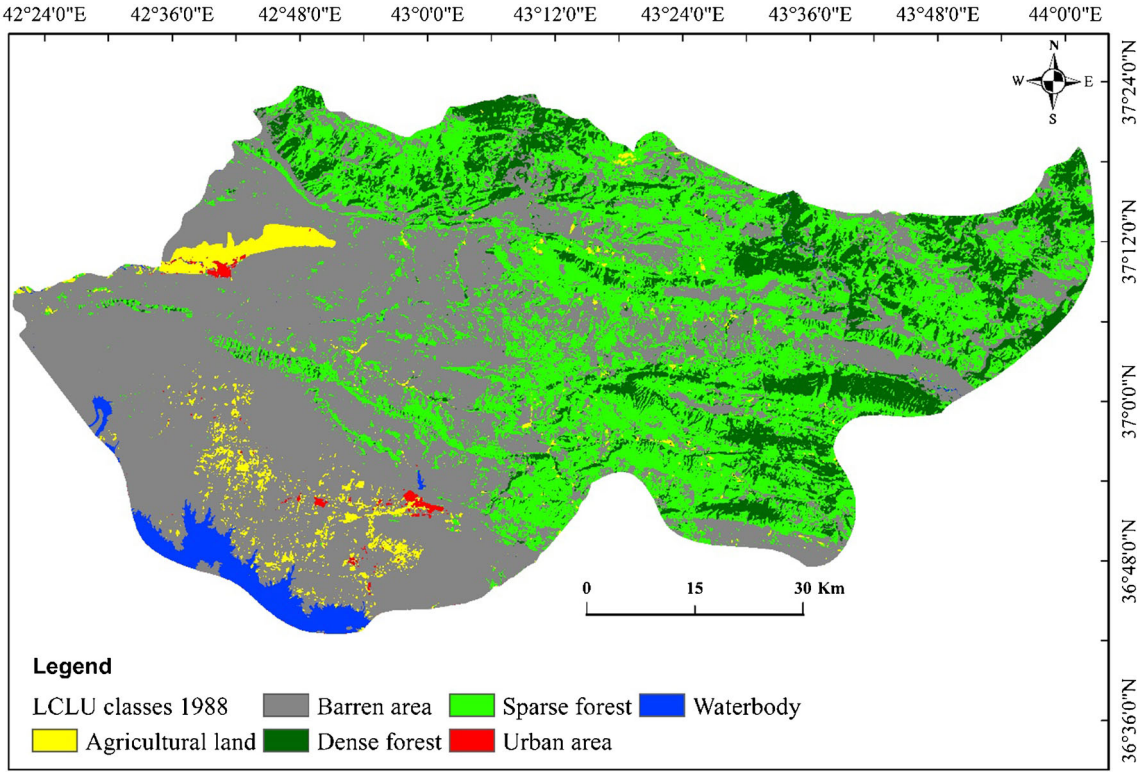

Fig. 3 Classified LULC map for 1988

(coefficient of determination) (Fig. 6). The statistical summary for other coefficient variations (kappa variations) for quantity and allocation agreement between the actual LULC map and the modelled LULC map) (Table 7) was Kno = 0.8315,

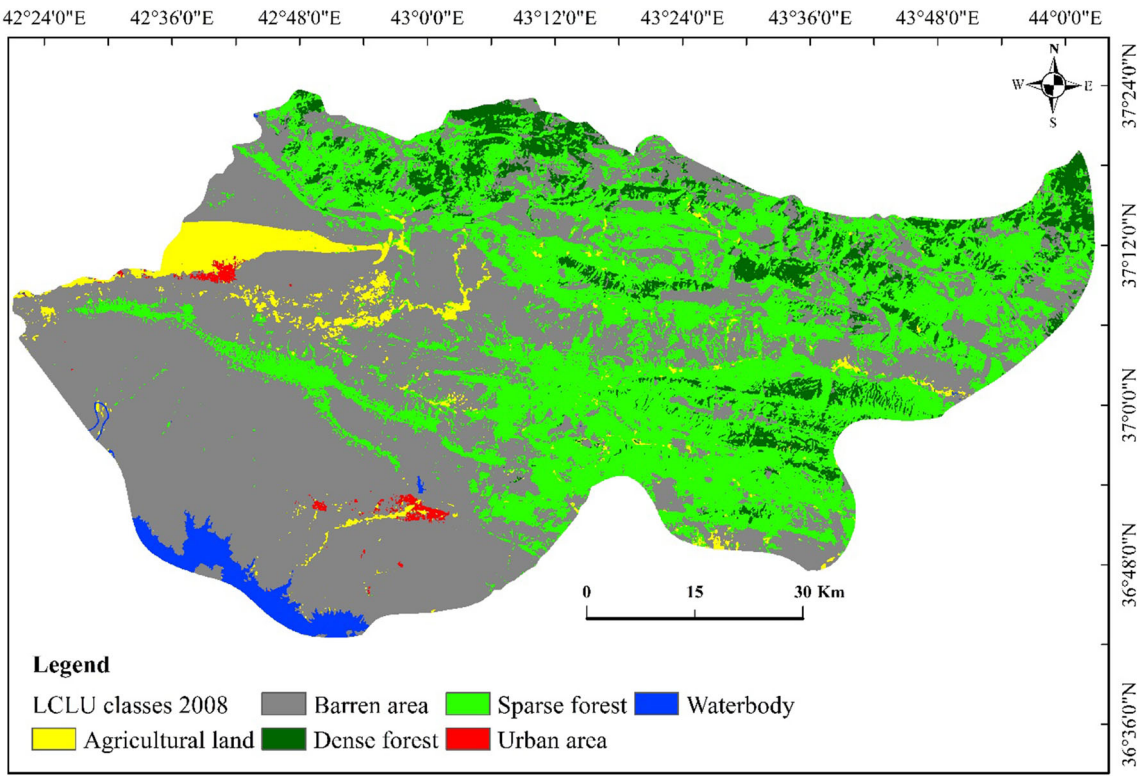

Fig. 4 Classified LULC map for 2008

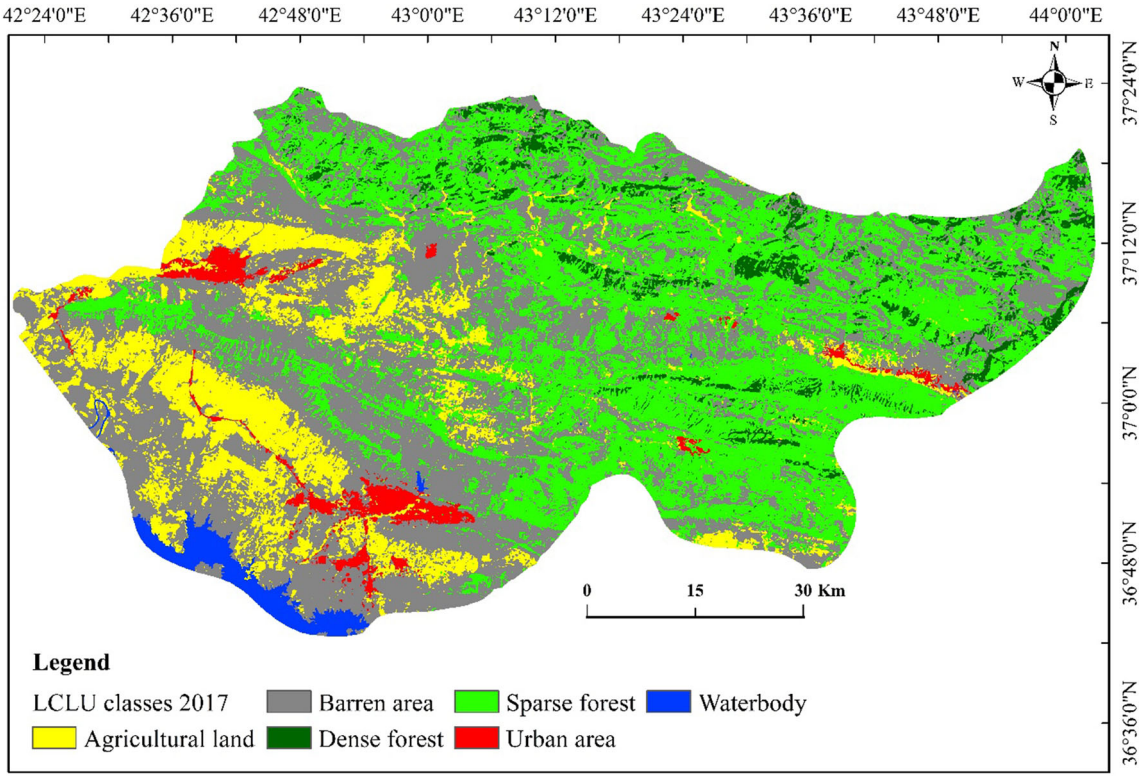

Fig. 5 Classified LULC map for 2017

Klocation = 0.8267, KlocationStrata = 0.8267 and Kstandard = 0.7978, respectively.

Predicting and mapping LULC changes

Figures 7 and 8 show the modelled LULC map for 2017 and LULC map for 2060, respectively. Future predictions demonstrated that between 2017 and 2060, dense forest, sparse forest, agricultural land and barren area will decrease approximately by −26.26% (from 327.08 to 241.08 km^2), −0.76% (from 2372.29 to 2355.82 km^2), −5.86% (from 973.21 to 916.27 km^2), −10.03% (from 2918.9 to 2626.19 km^2), respectively. Whereas, urban area and waterbody will increase approximately by 271.19%, (161.99 to 602.19.8 km^2), 10.4% (119.09 to 131.01 km^2), respectively (Table 6 and Fig. 9). The proportionality (probability percentage) of changes from one class category to another class is demonstrated in Table 8.

Discussion

In the study of environmental change, ecosystem integrity (e.g. structure and function), urban planning and sustainability, LULCC has become a key subject that needs to be

Table 3 Accuracy assessment (error matrix) for 1988

Class	Dense forest	Sparse forest	Agricultural land	Urban area	Barren area	Waterbody	Total	User accuracy
Dense forest	35	4	0	0	0	0	39	0.897
Sparse forest	6	33	0	0	0	0	39	0.846
Agricultural land	1	0	35	0	0	3	39	0.897
Urban area	0	0	0	35	4	0	39	0.897
Barren area	0	0	0	2	37	0	39	0.949
Waterbody	0	0	6	0	0	33	39	0.846
Total	42	37	41	37	41	36	234	0.000
Producer accuracy	0.833	0.892	0.854	0.946	0.902	0.917	0	0.889
Kappa	0.867							

Table 4 Accuracy assessment (error matrix) for 2008

Class	Dense forest	Sparse forest	Agricultural land	Urban area	Barren area	Water body	Total	User accuracy
Dense forest	36	3	0	0	0	0	39	0.923
Sparse forest	5	34	0	0	0	0	39	0.872
Agricultural land	0	0	39	0	0	0	39	1.000
Urban area	0	0	0	35	4	0	39	0.897
Barren area	2	0	0	2	35	0	39	0.897
Waterbody	0	0	0	0	4	35	39	0.897
Total	43	37	39	37	43	35	234	0.000
Producer accuracy	0.837	0.919	1.000	0.946	0.814	1	0	0.915
Kappa	0.897							

acknowledged and addressed. In this study, medium resolution satellite imagery from Landsat was used to derive LULC maps (i.e. 1988, 2008 and 2017) using the MLC. In addition, future LULC maps were predicted for year 2017 and 2060 using the synergy Cellular (CA)–Markov model, respectively. Historical socio-economic and instabilities have played some roles in selecting the time of the image acquisition. In 1988, Iraq just ceased 8 years of war with Iran and after that in 1991, Iraq was involved in Gulf war and followed by extensive economic sanctions by the United Nations (UN). Overall, six class categories were identified from the satellite imagery for the selected years. To train and validate the identified classes, two independent resources such as high-resolution Google Earth historical imagery and local expert knowledge were used. In places where resources are limited or access is restricted due to security issues, similar approaches were adopted to generate and validate LULC classification (Qader et al. 2016; Xie et al. 2019). These independent resources were effectively helped producing accurate classification outputs with relatively high Kappa index and user and producer accuracies. Therefore, accurate LULC maps can reliably be employed as a base for change analysis and prediction (Anderson 1976).

Interesting trends can be seen in the change statistics between 1988, 2008 and 2017. As shown in Table 6, a remarkable decrease was registered for the dense forest from 1988 to 2017. One of the main reasons for this loss could be harvesting the trees without replacing. Over the last few decades, Iraq and its people have suffered the consequences of an inactive economy and limited access to essential services because of successive sanctions, wars and sectarian conflicts (Martin 2018). These critical incidents resulted in burning vast areas of forests and forced thousands of people to migrate from rural areas to cities (Black 1993). In addition, other factors including farming, livestock feeding, mining and ploughing the forest soil might have caused forest destruction in this area. The consequences and negative impacts of these events could destruct further the spatial extent of dense forest in the future, as it can be seen in the model prediction for 2060 and the transition probability matrix. Dense forest would predominantly change to sparse forest (37%) and barren area (36%) respectively (Table 8), suggesting thinning and clearing activities. This

Table 5 Accuracy assessment (error matrix) for 2017

Class	Dense forest	Sparse forest	Agricultural land	Urban area	Barren area	Water body	Total	User accuracy
Dense forest	36	3	0	0	0	0	39	0.923
Sparse forest	2	37	0	0	0	0	39	0.949
Agricultural land	0	0	37	0	2	0	39	0.949
Urban area	0	0	0	35	4	0	39	0.897
Barren area	0	0	4	0	35	0	39	0.897
Waterbody	0	0	1	0	0	38	39	0.974
Total	38	40	42	35	41	38	234	0.000
Producer accuracy	0.947	0.925	0.881	1.000	0.854	1.000	0	0.932
Kappa	0.918							

Table 6 Change quantification (area percentage) for classified LULC and modelled LULC map from 1988 to 2060

	LULC 1988		LULC 2008		LULC 2017		LULC 2017 modelled		LULC 2060 modelled	
Class	Area km^2	%	Area km^2	%	Area km^2	%	Area km^2	%	Area km^2	%
Dense forest	860.99	12.53	491.55	7.15	327.08	4.76	260.03	3.78	241.08	3.51
Sparse forest	2071.78	30.15	2338.08	34.02	2372.29	34.52	2509.69	36.52	2355.82	34.28
Agricultural land	257.52	3.75	300.86	4.38	973.21	14.16	1124.45	16.36	916.27	13.33
Urban area	25.51	0.37	29.64	0.43	161.99	2.36	171.41	2.49	602.19	8.76
Barren area	3504.24	50.99	3589.38	52.23	2918.90	42.47	2715.11	39.51	2626.19	38.21
Waterbody	152.52	2.22	123.05	1.79	119.09	1.73	91.88	1.34	131.01	1.91
Total	6872.56	100	6872.56	100	6872.56	100	6872.56	100	6872.56	100

finding is consistent with other works in which similar trends were found (Chapman 1950; Khwarahm 2020; Mosa 2016). Oppositely, the area of sparse forest slightly increased as this class, in some circumstances, can be a transition stage between dense forest and other classes. Respectively, agricultural lands were increased with a clear jump in 2017. This is likely due to the influence of a recent policy that was implemented by the central government which have encouraged local farmers to increase agricultural production particularly wheat. Across Iraq, the central government has allocated silos to buy wheat from farmers for a pre-declared price above the market price (Jongerden et al. 2019).

The land use type that increased the most over the last four decades is urban area, which increased by six times from 0.37 to 2.36% (between 1988 and 2017). Similarly, a substantial increase can be seen in the predicted urban area for 2060. From 2017 to 2060, the increasing trend would be from 2.36 to 8.76% (almost four times). Agricultural land (by 14%) and barren area (by 11%) would have the highest probability of transition to urban area in 2060 (Table 6), suggesting urbanization shift towards new spatial extent and thus more disturbances. There are several possible explanations for this result. Increasing the population and development of infrastructure can result in accelerating urban expansion (Pandey and Khare 2017). Rapid population growth can be accounted as one of the main drivers of LULCCs. In the last two decades, like the rest of Middle East, Iraq and KRI have experienced significant population growth and partial economic growth. For instance, in four decades, population has increased from ~12.46 million to ~38.275 in Iraq (increased by 308% from 1977 to 2017) (UN 2017). This rapid population growth can be seen particularly in Duhok governorate due its close geographic location to Syria and ISIS occupied areas (e.g. Mosul). The Duhok governorate has a total population of 1.47 million as well as 718,000 displaced people (internally displaced persons (IDPs) and refugees aggregated) (UNHCR 2016). These IDPs and refugees have fled their home because of recent conflicts in Syria and Iraq and posed substantial pressure on urban expansion. In KRI, the majority of IDPs (80% of more than 1 million and refugees (60% out of 250,000) live in urban areas and sharing the scarce resources (UNHCR 2016). In addition, the economic progress after 2003 and the increase in the fiscal income from the central government during 2005–2013 from around $2.5 to $13 billion has promoted new economic

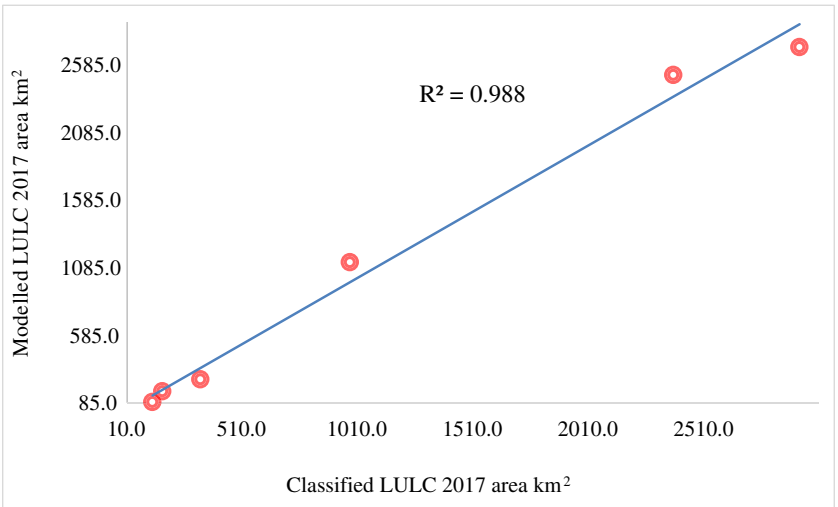

Fig. 6 Relationship between modelled and classified LULC maps for 2017

Table 7 Categorical comparison between classified LULC map 2017 and modelled LULC map 2017; the coefficient of Kappa variations for agreement and disagreement in quantity and allocation

	Information of quantity		
Information of allocation	No[n]	Medium[m]	Perfect[p]
Perfect[P(x)]	P(n) = 0.5611	P(m) = 0.9750	P(p) = 1.0000
PerfectStratum[K(x)]	K(n) = 0.5611	K(m) = 0.9750	K(p) = 1.0000
MediumGrid[M(x)]	M(n) = 0.4782	M(m) = 0.8556	M(p) = 0.8452
MediumStratum[H(x)]	H(n) = 0.1429	H(m) = 0.2859	H(p) = 0.2869
No[N(x)]	N(n) = 0.1429	N(m) = 0.2859	N(p) = 0.2869
AgreementChance = 0.1429			
AgreementQuantity = 0.1430			
AgreementStrata = 0.0000			
AgreementGridcell = 0.5697			
DisagreeGridcell = 0.1194			
DisagreeStrata = 0.0000			
DisagreeQuantity = 0.0250			
Kno = 0.8315			
Klocation = 0.8267			
KlocationStrata = 0.8267			
Kstandard = 0.7978			

planning and community development in KRI (Leezenberg 2015). In accordance with the present results, previous studies have demonstrated that urban area in Duhok has increased sprawl in all directions over last four decades (Hassan and Kotval-K 2019; Mohammed 2013).

With regard to the CA–Markov model validation, overall, there is a significant level of agreement between the predicted model outputs and LULC maps (Table 7). The Kappa statistical values are considered acceptable as far as the reliability of model variation is considered for further use (Landis and

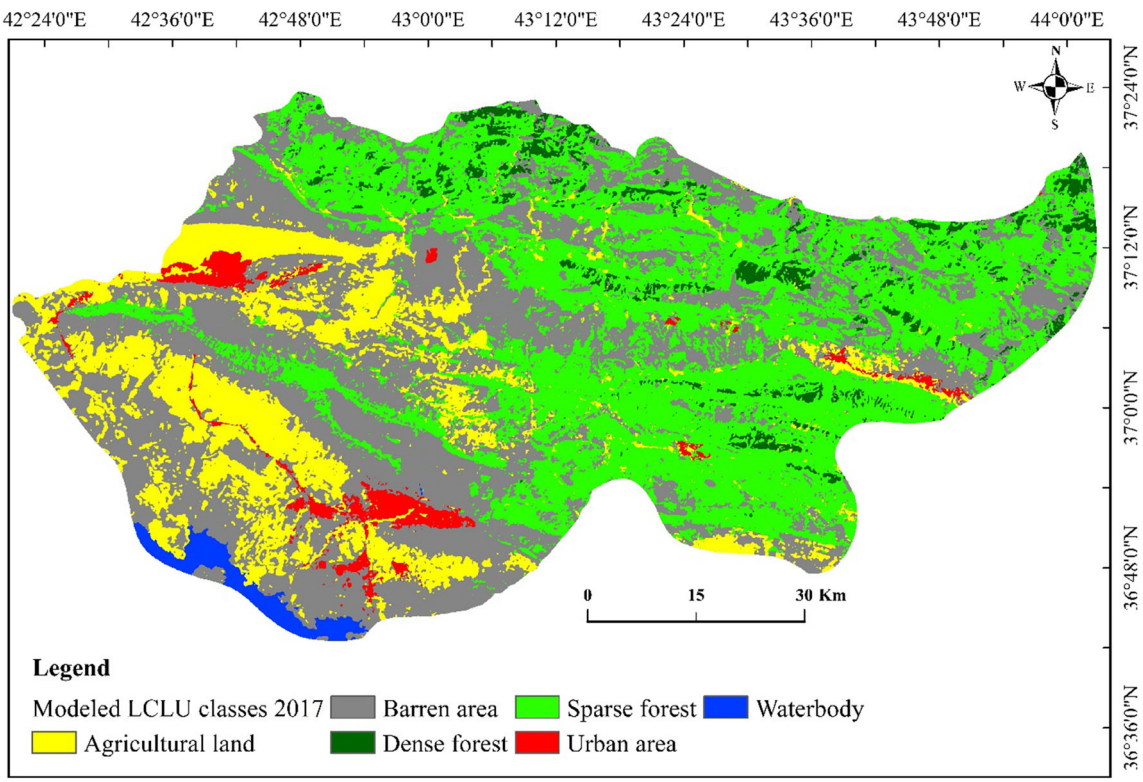

Fig. 7 Modelled LULC map for 2017

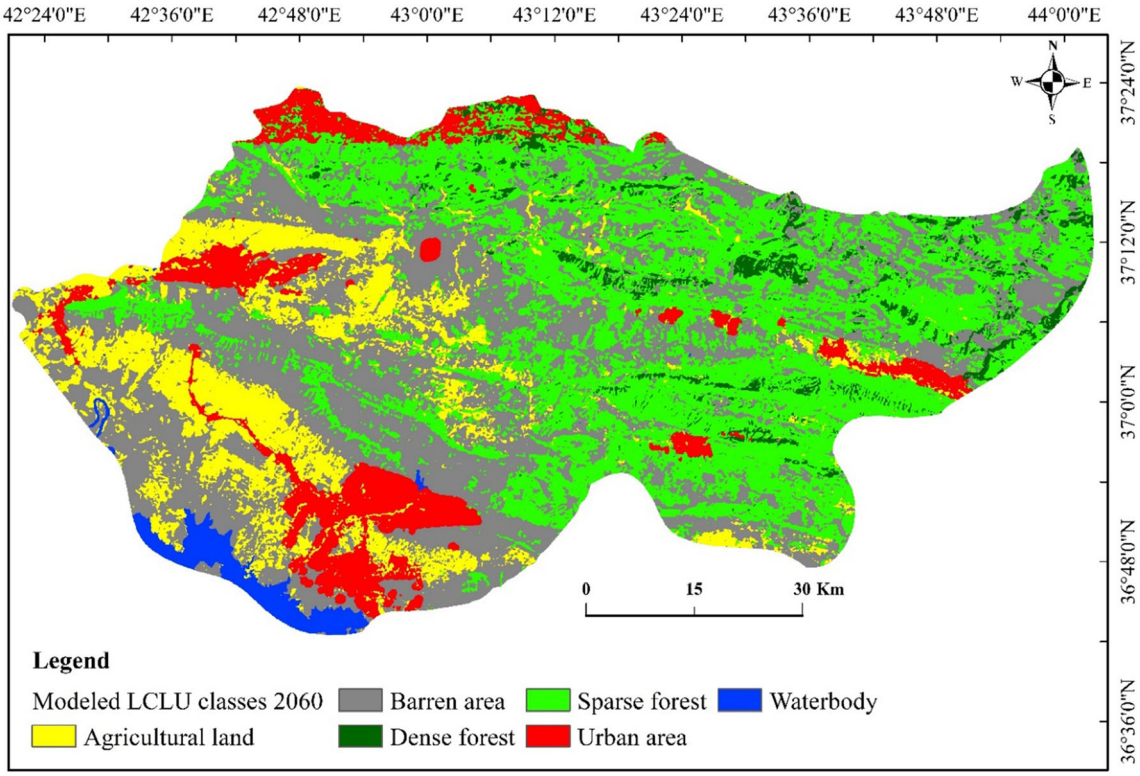

Fig. 8 Modelled LULC map for 2060

Koch 1977; Pontius Jr and Millones 2011). In some areas, the model might have underestimated the class areas, most likely due to the disagreement quantity value which in turn has impacted the overall model performance. In addition, the overall performance of the model in simulating future LULC maps for 2060 based on the transition probability matrix of 2017–2060 produced a reasonable accuracy (Table 7). Various values of Kappa coefficient variations for CA–Markov have been reported in literature (e.g. Kstandard of 0.68 (Hyandye and Martz 2017), 0.88 (Rimal et al. 2017), 0.59 Singh et al. (2018) and 0.95 (Munthali et al. 2020). In addition, in terms of area, the overall relationship between the modelled and classified maps, a co-efficient of determination value of (R^2 = 0.988) was obtained. This result is in line with study of Akbar et al. (2019), which reported the R^2 = 0.90 between the actual and modelled LULC maps.

Conclusion

Quantifying and predicting spatiotemporal dynamics of LULCCs have become a prerequisite for planning decisions and conserving the integrity of the ecosystems, particularly urban ecosystem as human population grows.

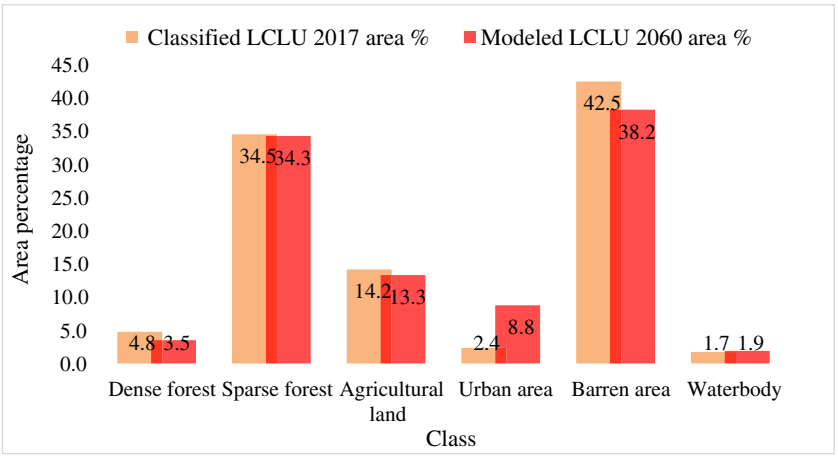

Fig. 9 LULCC dynamics between 2017 and 2060 years (area km^2 percentage)

Table 8 Transition matrix (probability percentage) of class category change from LULC map 2017 to LULC map 2060

Class	Dense forest	Sparse forest	Agricultural land	Urban area	Barren area	Waterbody
Dense forest	0.0415	0.3786	0.1687	0.0486	0.3604	0.0021
Sparse forest	0.0368	0.2966	0.1991	0.0651	0.3995	0.0029
Agricultural land	0.0266	0.2766	0.1904	0.1453	0.3529	0.0082
Urban area	0.0112	0.1247	0.198	0.4423	0.2123	0.0115
Barren area	0.0289	0.3081	0.2354	0.1166	0.3056	0.0054
Waterbody	0.0075	0.0739	0.0938	0.0352	0.1573	0.6322

Geospatial technologies together with land surface modellers (e.g. CA–Markov) are effective tools in providing invaluable information on the patterns of LCLCs over space and time. Understanding the patterns of changes would supply guidance to various scientific disciplines, for example, biodiversity conservation, sustainable urban systems and environmental management actions.

Dense forest in the Duhok governorate has seen remarkable decline from 1988 to 2017, and future predictions demonstrated that this trend would continue (i.e. from 2017 to 2060). Dense forest cover would predominantly convert to sparse forest and barren areas, suggesting forest thinning and clearing. Therefore, management actions should focus on protecting the forest areas as part of the sustainable development. Moreover, the most dynamic land use type that increased the most over the last four decades was urban area, which increased by six times from 0.37 to 2.36% (between 1988 and 2017). Future predictions demonstrated that this trend would continue to increase from 2.36% (2017) to 8.76% (2060) (i.e. by almost four times). Urbanization would continue to increase predominantly at the cost of agricultural land and barren area.

Acknowledgements We would like to thank the United States Geological Survey (USGS) to make the Earth Observation data freely available. The support and assistance of the University of Sulaimani, in particular, Department of Biology is highly appreciated. We also would like to thank the anonymous reviewers for their valuable comments and feedback.

Funding Not applicable.

Data availability Not applicable.

Code availability Not applicable.

Declarations

Conflicts of interest/Competing interests The authors declare no competing interests.

References

Abdullahi S, Pradhan B (2016) Sustainable brownfields land use change modeling using GIS-Based weights-of-evidence approach Applied spatial analysis and policy 9:21-38

Abdullahi S, Pradhan B, Mansor S, Shariff ARM (2015) GIS-based modeling for the spatial measurement and evaluation of mixed land use development for a compact city GIScience & Remote Sensing 52:18-39

Agha OMAM, Şarlak N (2016) Spatial and temporal patterns of climate variables in Iraq. Arab J Geosci 9:9. https://doi.org/10.1007/s12517-016-2324-y

Akbar TA, Hassan QK, Ishaq S, Batool M, Butt HJ, Jabbar H (2019) Investigative spatial distribution and modelling of existing and future urban land changes and its impact on urbanization and economy. Remote Sens 11:105

Al-sharif AA, Pradhan B (2015) A novel approach for predicting the spatial patterns of urban expansion by combining the chi-squared automatic integration detection decision tree, Markov chain and cellular automata models in GIS Geocarto International 30:858-881

Al-sharif AA, Pradhan B (2016) Spatio-temporal prediction of urban expansion using bivariate statistical models: assessment of the efficacy of evidential belief functions and frequency ratio models. Appl Spat Anal Policy 9:213–231

Alkaradaghi K, Ali SS, Al-Ansari N, Laue J (2018) Evaluation of land use & land cover change using multi-temporal landsat imagery: a case study Sulaimaniyah Governorate, Iraq. J Geogr Inf Syst 10: 247–260

Alsharif AA, Pradhan B (2014) Urban sprawl analysis of Tripoli Metropolitan city (Libya) using remote sensing data and multivariate logistic regression model. J Indian Soc Remote Sens 42:149–163

Alsharif AA, Pradhan B, Mansor S, Shafri HZM (2015) Urban expansion assessment by using remotely sensed data and the relative Shannon entropy model in GIS: a case study of Tripoli, Libya Theoretical and Empirical Researches in Urban Management 10:55-71

Anderson JR (1976) A land use and land cover classification system for use with remote sensor data vol 964. US Government Printing Office

Arneth A et al. (2019) IPCC special report on climate change, desertification, land degradation, sustainable land management, food security, and greenhouse gas fluxes in terrestrial ecosystems Summary for Policy Makers Geneva: Intergovernmental Panel on Climate Change (IPCC)

Barredo JI, Demicheli L (2003) Urban sustainability in developing countries' megacities: modelling and predicting future urban growth in Lagos Cities 20:297-310

Black G (1993) Genocide in Iraq: the Anfal campaign against the Kurds. Human Rights Watch,

Butt A, Shabbir R, Ahmad SS, Aziz N (2015) Land use change mapping and analysis using Remote Sensing and GIS: a case study of Simly watershed, Islamabad, Pakistan The Egyptian Journal of Remote Sensing and Space Science 18:251-259

Chapman G (1950) Notes on forestry in Iraq Empire Forestry Review: 132-135

Chen J (2007) Rapid urbanization in China: a real challenge to soil protection and food security. Catena 69:1–15

Christensen M, Jokar Arsanjani J (2020) Stimulating implementation of sustainable development goals and conservation action: predicting future land use/cover change in Virunga National Park, Congo. Sustainability 12:1570

Congalton RG, Green K (2019) Assessing the accuracy of remotely sensed data: principles and practices. CRC press

Corner RJ, Dewan AM, Chakma S (2014) Monitoring and prediction of land-use and land-cover (LULC) change. Dhaka megacity. Springer, In, pp 75–97

Dbehera M, Borate SN, Panda SN, Behera PR, Roy PS (2012) Modelling and analyzing the watershed dynamics using Cellular Automata (CA)–Markov model–a geo-information based approach Journal of earth system science 121:1011-1024

Dewan AM, Yamaguchi Y (2009) Land use and land cover change in Greater Dhaka, Bangladesh: using remote sensing to promote sustainable urbanization. Appl Geogr 29:390–401

Dibs H, Hasab HA, Al-Rifaie JK, Al-Ansari N (2020) An optimal approach for land-use/land-cover mapping by integration and fusion of multispectral landsat OLI images: case study in Baghdad. Iraq Water, Air, & Soil Pollution 231:1–15

Eastman J (2012) IDRISI selva: guide to GIS and image processing Clark Labratories, Clark University, Worcester, Massachusetts, USA

Foody GM (2002) Status of land cover classification accuracy assessment. Remote Sens Environ 80:185–201

Gibson GR, Campbell JB, Zipper CE (2015) Sociopolitical influences on cropland area change in Iraq, 2001–2012 Appl Geogr 62:339-346

Gómez C, White JC, Wulder MA (2016) Optical remotely sensed time series data for land cover classification: a review ISPRS Journal of Photogrammetry and Remote Sensing 116:55-72

Guan D, Li H, Inohae T, Su W, Nagaie T, Hokao K (2011) Modeling urban land use change by the integration of cellular automaton and Markov model Ecological Modelling 222:3761-3772

Habitat U, ESCAP U (2015) The state of Asian and Pacific cities 2015: urban transformations shifting from quantity to quality UN Habitat, London, UK

Hadeel A, Jabbar MT, Chen X (2010) Environmental change monitoring in the arid and semi-arid regions: a case study Al-Basrah Province, Iraq. Environ Monit Assess 167:371–385

Hadi SJ, Shafri HZ, Mahir MD (2014) Modelling LULC for the period 2010-2030 using GIS and Remote sensing: a case study of Tikrit, Iraq. In: IOP conference series: earth and environmental science, vol 1. IOP Publishing, p 012053

Hasanlou M, Seydi ST, Shah-Hosseini R (2018) A sub-pixel multiple change detection approach for hyperspectral imagery. Can J Remote Sens 44:601–615

Hassan A, Kotval-K Z (2019) A Framework for measuring urban sustainability in an emerging region: the City of Duhok as a case study. Sustainability 11:11. https://doi.org/10.3390/su11195402

He D, Zhou J, Gao W, Guo H, Yu S, Liu Y (2014) An integrated CA-markov model for dynamic simulation of land use change in Lake Dianchi watershed Acta Scientiarum Naturalium Universitatis Pekinensis 50:1095-1105

Hyandye C, Mandara CG, Safari J (2015) GIS and logit regression model applications in land use/land cover change and distribution in Usangu catchment American Journal of Remote Sensing 3:6-16

Hyandye C, Martz LW (2017) A Markovian and cellular automata land-use change predictive model of the Usangu Catchment International journal of remote sensing 38:64-81

Ibrahim F, Rasul G (2017) Urban land use land cover changes and their effect on land surface temperature: case study using Dohuk City in the Kurdistan Region of Iraq Climate 5:13

Jensen JR (1996) Introductory digital image processing: a remote sensing perspective, vol Ed. 2. Prentice-Hall Inc.

Jongerden J, Wolters W, Dijkxhoorn Y, Gur F, Ozturk M (2019) The politics of agricultural development in Iraq and the Kurdistan Region in Iraq (KRI). Sustainability 11:11. https://doi.org/10.3390/su11215874

Karki S, Thandar AM, Uddin K, Tun S, Aye WM, Aryal K, Kandel P, Chettri N (2018) Impact of land use land cover change on ecosystem services: a comparative analysis on observed data and people's perception in Inle Lake, Myanmar. Environ Syst Res 7:25

Khwarahm NR (2020) Mapping current and potential future distributions of the oak tree (Quercus aegilops) in the Kurdistan Region. Iraq Ecological Processes 9:1–16

Khwarahm NR (2021) Spatial modeling of land use and land cover change in Sulaimani, Iraq, using multitemporal satellite data. Environ Monit Assess 193:1–18

Khwarahm NR, Ararat K, Qader S, Al-Quraishi AMF (2021a) Modelling habitat suitability for the breeding Egyptian vulture (*Neophron percnopterus*) in the Kurdistan Region of Iraq Iranian Journal of Science and Technology, Transactions A: Science:1-12

Khwarahm NR, Ararat K, Qader S, Sabir DK (2021b) Modeling the distribution of the Near Eastern fire salamander (*Salamandra infraimmaculata*) and Kurdistan newt (*Neurergus derjugini*) under current and future climate conditions in Iraq. Ecol Inform 63:101309

Khwarahm NR, Qader S, Ararat K, Al-Quraishi AMF (2020) Predicting and mapping land cover/land use changes in Erbil/Iraq using CA-Markov synergy model Earth Science Informatics:1-14

Koomen E, Borsboom-van Beurden J (2011) Land-use modelling in planning practice. Springer Nature,

Kulaksiz S (2015) Kurdistan regional government: economic and social impact assessment of the Syrian conflict and ISIS insurgency

Lambin EF, Meyfroidt P (2011) Global land use change, economic globalization, and the looming land scarcity Proceedings of the National Academy of Sciences 108:3465-3472

Landis JR, Koch GG (1977) The measurement of observer agreement for categorical data biometrics:159-174

Leezenberg M (2015) Politics, economy, and ideology in Iraqi Kurdistan since 2003: enduring trends and novel challenges. Arab Stud J 23: 154–183

Li W, Dong R, Fu H, Wang J, Yu L, Gong P (2020) Integrating Google Earth imagery with Landsat data to improve 30-m resolution land cover mapping. Remote Sens Environ 237:111563

Liang S, Fang H, Morisette JT, Chen M, Shuey CJ, Walthall CL, Daughtry CS (2002) Atmospheric correction of Landsat ETM+ land surface imagery. II Validation and applications IEEE transactions on Geoscience and Remote Sensing 40:2736-2746

Liping C, Yujun S, Saeed S (2018) Monitoring and predicting land use and land cover changes using remote sensing and GIS techniques—a case study of a hilly area, Jiangle, China. PLoS One 13:e0200493

Martin K (2018) Syria and Iraq ISIS and other actors in historical context. Feisal al-Istrabadi and Sumit Ganguly (2018) The future of ISIS: Regional …,

Mishra VN, Rai PK (2016) A remote sensing aided multi-layer perceptron-Markov chain analysis for land use and land cover change prediction in Patna district (Bihar), India. Arab J Geosci 9: 249

Mohammed J (2013) Rapid urban growth in the city of Duhok, Iraqi Kurdistan Region: an integrated approach of GIS, remote sensing and Shannon entropy application. Int J Geomat Geosci 4:325

Mosa WL (2016) Forest cover change and migration in Iraqi Kurdistan: a case study from Zawita Sub-district. Michigan State University, Forestry

Munthali M, Mustak S, Adeola A, Botai J, Singh S, Davis N (2020) Modelling land use and land cover dynamics of Dedza district of Malawi using hybrid Cellular Automata and Markov model Remote Sensing Applications: Society and Environment 17:100276

Najmaddin PM (2017) Simulating river runoff and terrestrial water storage variability in data-scarce semi-arid catchments using remote sensing. University of Leicester

Natali D (2013) The Kurdistan Region of Iraq: stabilizer or spoiler? Georgetown Journal of International Affairs:71-79

Ouyang Z, Fan P, Chen J (2016) Urban built-up areas in transitional economies of Southeast Asia: spatial extent and dynamics. Remote Sens 8:819

Pandey BK, Khare D (2017) Analyzing and modeling of a large river basin dynamics applying integrated cellular automata and Markov model. Environ Earth Sci 76:1–12

Parsa VA, Yavari A, Nejadi A (2016) Spatio-temporal analysis of land use/land cover pattern changes in Arasbaran Biosphere Reserve: Iran Modeling Earth Systems and Environment 2:1-13

Pflugmacher D, Rabe A, Peters M, Hostert P (2019) Mapping pan-European land cover using Landsat spectral-temporal metrics and the European LUCAS survey. Remote Sens Environ 221:583–595

Pontius GR, Malanson J (2005) Comparison of the structure and accuracy of two land change models. Int J Geogr Inf Sci 19:243–265

Pontius RG Jr (2000) Comparison of categorical maps. Photogramm Eng Remote Sens 66:1011–1016

Pontius RG Jr (2002) Statistical methods to partition effects of quantity and location during comparison of categorical maps at multiple resolutions. Photogramm Eng Remote Sens 68:1041–1050

Pontius RG Jr, Cheuk ML (2006) A generalized cross-tabulation matrix to compare soft-classified maps at multiple resolutions. Int J Geogr Inf Sci 20:1–30

Pontius RG Jr, Millones M (2011) Death to Kappa: birth of quantity disagreement and allocation disagreement for accuracy assessment. Int J Remote Sens 32:4407–4429

Qader SH, Dash J, Atkinson PM, Rodriguez-Galiano V (2016) Classification of vegetation type in Iraq using satellite-based phenological parameters Ieee Journal of Selected Topics in Applied Earth Observations and Remote Sensing 9:414-424 https://doi.org/10.1109/jstars.2015.2508639

Ramankutty N, Foley JA (1999) Estimating historical changes in global land cover: Croplands from 1700 to 1992 Glob Biogeochem Cycles 13:997-1027

Rimal B, Zhang L, Keshtkar H, Haack BN, Rijal S, Zhang P (2018) Land use/land cover dynamics and modeling of urban land expansion by the integration of cellular automata and markov chain. ISPRS Int J Geo Inf 7:154

Rimal B, Zhang L, Keshtkar H, Wang N, Lin Y (2017) Monitoring and modeling of spatiotemporal urban expansion and land-use/land-cover change using integrated Markov chain cellular automata model. ISPRS Int J Geo Inf 6:288

Rosenfield GH (1986) Analysis of thematic map classification error matrices. Photogramm Eng Remote Sens 52:681–686

Sayemuzzaman M, Jha M (2014) Modeling of future land cover land use change in North Carolina using Markov chain and cellular automata model. Am J Eng Appl Sci 7:295

Seydi ST, Hasanlou M, Amani M (2020) A new end-to-end multi-dimensional CNN framework for land cover/land use change detection in multi-source remote sensing datasets. Remote Sens 12:2010

Singh SK, Laari PB, Mustak S, Srivastava PK, Szabó S (2018) Modelling of land use land cover change using earth observation data-sets of Tons River Basin, Madhya Pradesh, India Geocarto international 33:1202-1222

Su S, Xiao R, Jiang Z, Zhang Y (2012) Characterizing landscape pattern and ecosystem service value changes for urbanization impacts at an eco-regional scale. Appl Geogr 34:295–305

Tan M, Li X, Xie H, Lu C (2005) Urban land expansion and arable land loss in China—a case study of Beijing–Tianjin–Hebei region Land use policy 22:187-196

Tolessa T, Senbeta F, Kidane M (2017) The impact of land use/land cover change on ecosystem services in the central highlands of Ethiopia Ecosystem services 23:47-54

UN (2017) World population prospects: the 2017 revision, key findings and advance tables Department of Economics and Social Affairs PD, editor New York: United Nations

United Nations High Commissioner for Refugees (UNHCR) (2016) Displacement as challenge and opportunity Urban profile: Refugees, internally displaced persons and host community Duhok Governorate, Kurdistan Region of Iraq August 2016. Retrieved December 30, 2020 from https://reliefweb.int/sites/reliefweb.int/files/resources/DuhokUrbanProfileRefugeesIDPsandHostCommunityEnglishVersionUNHCRandDSONov.2016.pdf

Van Oort P (2007) Interpreting the change detection error matrix. Remote Sens Environ 108:1–8

Wang SW, Gebru BM, Lamchin M, Kayastha RB, Lee W-K (2020) Land use and land cover change detection and prediction in the Kathmandu District of Nepal using remote sensing and GIS. sustainability 12:3925

Wu J, Jenerette GD, Buyantuyev A, Redman CL (2011) Quantifying spatiotemporal patterns of urbanization: the case of the two fastest growing metropolitan regions in the United States Ecological Complexity 8:1-8

Wu W, Zhao S, Zhu C, Jiang J (2015) A comparative study of urban expansion in Beijing, Tianjin and Shijiazhuang over the past three decades. Landsc Urban Plan 134:93–106

Xie S, Liu LY, Zhang X, Yang JN, Chen XD, Gao Y (2019) Automatic land-cover mapping using Landsat time-series data based on Google Earth Engine. Remote Sens 11:11. https://doi.org/10.3390/rs11243023

Xu Y, Chan EH, Yung EH (2015) Overwhelming farmland conversion for urban development in transitional China: case study of Shanghai. Journal of Urban Planning and Development 141:05014013

Yang X, Zheng X-Q, Lv L-N (2012) A spatiotemporal model of land use change based on ant colony optimization, Markov chain and cellular automata. Ecol Model 233:11–19

Zhu Z, Woodcock CE (2014) Continuous change detection and classification of land cover using all available Landsat data Remote sensing of Environment 144:152-171